

Learning and Recognition in Excitable Chemical Reactor Networks

W. Hohmann, M. Kraus, and F. W. Schneider*

Institute of Physical Chemistry, University of Würzburg, Am Hubland, 97074 Würzburg, Germany

Received: December 2, 1997; In Final Form: January 21, 1998

In further work on recognition and learning we present a reactor network consisting of four electrically coupled chemical reactors that are connected via Pt working electrodes in the fashion of a Hopfield network. Each reactor can assume either a periodic (P) or a nodal (N) state in the Belousov–Zhabotinsky (BZ) reaction. Two out of 16 (2^4) dynamical patterns are encoded by local coupling. The encoded patterns have been chosen such that their Hopfield matrix shows both positive and negative coupling strengths. To successfully recognize all remaining (14) patterns, an averaging procedure for all amplitudes was introduced. Numerical simulations using the seven-variable Györgyi–Field model for the BZ reaction are in good agreement with the recognition experiments. We also simulate an iterative learning method to build up the synaptic strengths from a random Hopfield matrix without any back-propagation of errors. Recognition occurs abruptly at a certain number of iterations in the absence of any noise reminiscent of a phase transition. The inclusion of parameter noise is found to always broaden the recognition probability. Parameter noise enhances the recognition of patterns in the early iteration stages, while the recognition probability is drastically reduced in the later stages of iterative learning.

Introduction

The motivation for the present work is our fascination with physicochemical systems that are able to perform logic functions^{1,2} or to learn and to recognize dynamical patterns.^{3–8} Physicochemical learning and recognition devices must be networks composed of chemical subsystems (e.g., chemical reactors) that are coupled in specific ways. In previous studies we described the recognition and nonrecognition of chemical oscillation patterns with a reactor network consisting of four identical chemical reactors that were locally and globally coupled by Pt working electrodes. All four reactors were run in oscillatory states of the Belousov–Zhabotinsky (BZ) reaction. The oscillatory patterns were reached either from a focal steady state³ or from a nodal steady state⁴ using an external periodic perturbation with the electrical current as the bifurcation parameter. The encoded patterns consisted of in-phase⁴ (positive coupling) or out-of-phase oscillations³ (negative coupling), and all frequencies were practically identical. Without the entraining effect of global coupling the experimental oscillatory patterns eventually lose their phases and become destabilized. If each reactor is coupled with any of the other reactors, the network will be similar to a Hopfield network which is capable of performing the task of association; it associates (recognizes) a presented pattern of reactor states with a pattern that it has learned before.

In this work we reduce the complexity of the system by excluding global coupling altogether and by using local coupling only. Each reactor in the network must be in one of two dynamical states. The transition between the two states should not be gradual but sharp for efficient operation. In a distant analogy with in vivo neurons and axons⁹ we chose an oscillatory state denoted by the symbol P (periodic) and a steady state denoted by N (nodal) in this work for the two dynamical states. The Belousov–Zhabotinsky (BZ) reaction serves as the two-state chemical reaction, although other nonlinear reactions would do as well. Here the process of recognition involves the

transformations between the two reactor states P and N. As described earlier⁴ an increase of an applied electrical current as the bifurcation parameter will change a P state into a N state via a saddle node infinite period bifurcation (SNIPER) in the BZ reaction. Thus the high-current node is excitable since a (negative) pulse of the electric current will move the system across its bifurcation (SNIPER) point into the oscillatory region with a large oscillatory excursion. Therefore, the application of a current to the Pt working electrode of a BZ reactor will determine whether a reactor is in its oscillatory P or in a high-current excitatory N state.

In a Hopfield net, learning is a one-step process that consists of calculating a coupling matrix from the patterns to be encoded.¹⁰ The resulting 4×4 matrix (four-reactor network) may contain positive and/or negative coupling strengths depending on whether a given coupling interaction is positive or negative. Positive coupling is attractive, i.e., it will drive two coupled reactors into identical dynamic states, whereas negative coupling is repulsive, driving the reactors into opposite states. However, when both positive and negative couplings are present in the Hopfield matrix for a given encoded pattern, the situation becomes complicated since both transformations $N \rightarrow P$ and $P \rightarrow N$ may be required in the recognition process. In this work we have solved the problem of simultaneous positive and negative coupling in the absence of global coupling by first averaging over one or more oscillations in a P state and using the averaged (and not the oscillatory) signal as the weighted input to the other reactors. With this averaging procedure, which covers periodic as well as nodal states, any pattern is recognized even in the absence of global coupling. Furthermore, any phase relations are no longer required.

Learning by Iterative Self-Encoding in a Hopfield Net. Instead of using the traditional one-step learning procedure^{10,11} it is possible to let our small reactor network learn patterns by self-encoding its Hopfield matrix in many small steps. This is demonstrated by computer experiments in this work. We

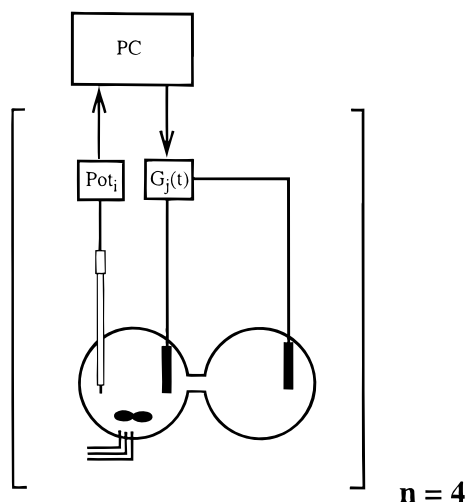


Figure 1. Four CSTRs ($n = 4$) of the type given here, each connected to their reference reactors via Teflon membranes. The redox potentials Pot_i are monitored by Pt/Ag/AgCl redox electrodes. The electric currents $G_j(t)$ (eq 3) are applied via galvanostats to the Pt working electrodes inserted in each reactor.

achieve self-encoding by a repetitive presentations of the same patterns. This simple procedure facilitates the inclusion of noise in a straightforward manner. Each time a pattern is presented to the network, the relevant coupling strengths in the Hopfield matrix are augmented or lowered by the same increments according to a Hebbian learning rule.¹² This learning method works even in the presence of spurious other patterns that, however, are presented less often. After each single learning iteration, a recognition experiment is carried out as a check. When the network has recognized a pattern after a given number of iterations has taken place, the learning process is considered as successful. In the absence of any or little noise, it will be observed that recognition occurs abruptly from one iteration to the next after a minimum number of iterations have been carried out. Therefore a threshold exists that leads to a sharp “phase transition”: below threshold there is nonrecognition and above threshold every single recognition event is successful. No further optimization procedure such as back-propagation of errors^{13,14} is necessary.

We shall show that learning from random weights (synapses) by the inclusion of parameter noise in the coupling strengths generates a broadened but lowered recognition curve, and the probability of recognition is nonzero at a substantially lower number of iteration cycles than in the absence of noise. For this reason large noise turns out to be advantageous only in the early stages of learning since it dramatically increases the probability of recognition at a lower number of iterations. On the other hand, strong noise is detrimental in the subsequent stages of learning where the noise-free system has achieved full recognition. In the latter case, a repetitive addition of noise decreases the probability of recognition by “forgetting”, i.e., by randomizing all coupling strengths (elements) in the Hopfield matrix.

Experimental Section

Four CSTRs (continuous flow stirred tank reactors) of 4.2 mL volume each are connected to their reference reactors via Teflon membranes (Figure 1). Three reactant feed streams into each CSTR are delivered by precise piston pumps at identical rates with three syringes (50 mL each), where syringe I delivers 0.42 mol/L NaBrO_3 ; syringe II, 1.5×10^{-3} mol/L $\text{Ce}_2(\text{SO}_4)_3$

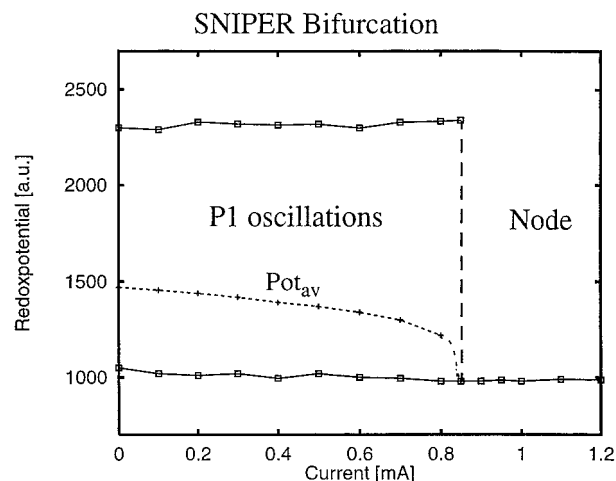


Figure 2. Experimental bifurcation diagram with a SNIPER bifurcation at 0.85 mA using the electrical current as the bifurcation parameter at $k_f = 6.0 \times 10^{-4} \text{ s}^{-1}$. The P1 oscillations of the free running system change into a nodal steady state at the SNIPER bifurcation. The amplitudes of the P1 oscillations remain almost constant, while the averaged redox potential decreases from 1450 arb. units to 1000 arb. units at the SNIPER bifurcation.

and 0.9 mol/L malonic acid; and syringe III, 1.125 mol/L sulfuric acid. The flow rate was fixed at $k_f = 6.0 \times 10^{-4} \text{ s}^{-1}$ (residence time 27.8 min) in order to establish stable P1 oscillations. The outflow was pumped off at the top of each CSTR. The reference reactors contain 0.4 mol/L sulfuric acid. Reactors, feed lines, and syringes are thermostated at 25 °C; Teflon-coated magnetic stirrers operate at 1000 rpm. The redox potentials Pot_i in each CSTR are measured by Pt/Ag/AgCl redox electrodes and digitally monitored at 1 Hz. Owing to variations in the sensitivities of the redox electrodes, the normalized redox potentials are presented in arbitrary units. Electrical coupling is performed by applying an electrical current $G_j(t)$ to the Pt working electrodes inserted in each reactor. The electrical current is controlled by galvanostats (E&G Instruments) according to eq 3. In the recognition phase all currents are reevaluated every second: the output ($Pot_{i,av}$) affects the next input ($G_j(t)$) in a cyclic fashion until the network is stabilized at a given pattern after a short transience of ~ 1 oscillation has elapsed.

SNIPER Bifurcation. When currents higher than 0.85 mA are applied to the Pt working electrode (Figure 2), the BZ oscillations change into a nodal steady state when $k_f = 6.0 \times 10^{-4} \text{ s}^{-1}$. Thereby the period of the BZ oscillations increases from 30 s to ~ 1000 s as the current approaches the bifurcation point, demonstrating a so-called SNIPER (saddle node infinite period) bifurcation (see also ref 4). The amplitudes of the oscillations remain almost constant up to the SNIPER point, where they collapse to zero. The signals of the redox electrodes were arbitrarily set to 1000 au at the steady state, which is the reference state. The steady-state region displays a practically constant potential independent of the current. The calculated average value of the redox potential Pot_{av} in the P regime decreases slightly with increasing currents in the neighborhood of the SNIPER bifurcation point (Figure 2).

Before the start of a coupling experiment all electrical currents (G_{1in} to G_{4in}) are set to 0.45 or 1.05 mA in order to establish either oscillations (P) or a nodal steady state (N), respectively, as initial conditions. For four reactors all (16) possible oscillation patterns are listed in Figure 3.

Hopfield Network. A Hopfield network uses a simple matrix notation to describe the coupling strengths between the indi-

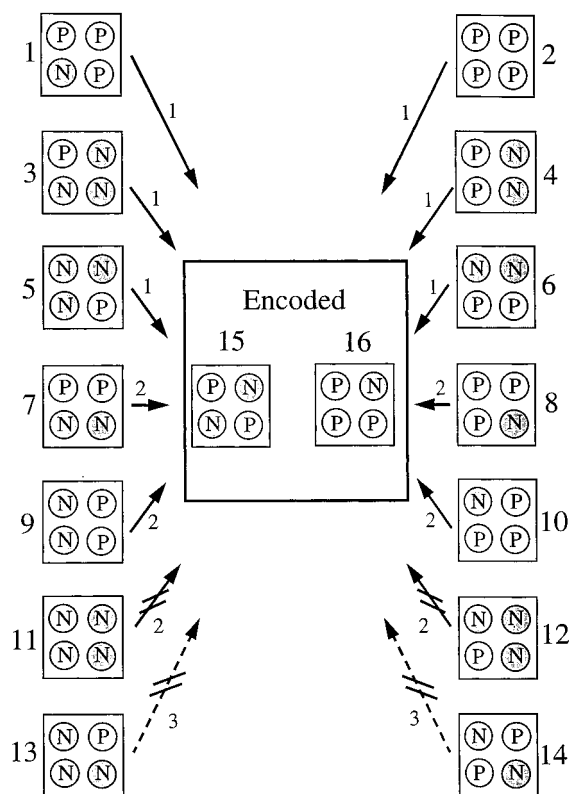


Figure 3. Four reactors showing 16 possible oscillation patterns (numbered) where P (N) stands for a periodic (nodal) state. The number of errors with respect to the encoded patterns 15 and 16 is indicated close to the arrows. For all initial patterns (except patterns 11 and 12) recognition is achieved. Patterns 13 and 14 are mirror images of patterns 16 and 15, respectively, as indicated by broken arrows. The numbering of the four reactors is given in the coupling scheme (see text).

vidual units, where, in principle, each unit may be connected to any of the other units. Hopfield nets are able to recognize encoded patterns if the presented patterns contain relatively few errors with respect to the encoded patterns. If there are more than 50% errors, the network recognizes the mirror images of the encoded patterns.

To establish a Hopfield matrix, one may use a bipolar notation for a single interaction. We use +1 for the notation of a periodic state and -1 for a nodal steady state. The coupling weights w_{ij} between reactor i and j are calculated as the sum of the products of two interacting states, where p is the number of patterns to be encoded:

$$w_{ij} = \sum_{s=1}^p x_i^s x_j^s \quad \text{for } i \neq j \quad (1)$$

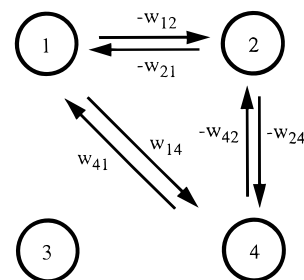
$$w_{ij} = 0 \quad \text{for } i = j \quad (2)$$

In other words, if two coupled reactors are in the same state (i.e., both in the oscillatory or both in the steady states), the product of their statistical weights is always +1 (positive); if the two states are unlike, the product of their statistical weights is always -1 (negative). For several encoded patterns the individual statistical weight products are simply added and the sum is entered into the Hopfield matrix. In previous work³ we used only negative entries, since the stored patterns were out-of-phase by 180°, or, later,⁴ positive entries, because all stored patterns involved only in-phase oscillatory states. The weights of the Hopfield matrix are calculated (learned) in one step for all patterns to be encoded. In subsequent recognition experiments these weights do not change.

Encoding Patterns 15 and 16. As an example, we encode patterns 15 and 16 (Figure 3). These were chosen because their Hopfield matrix \mathbf{W} contains positive as well as negative w_{ij} values (coupling constants). \mathbf{W} is identical for the corresponding mirror images 13 and 14:

$$\mathbf{W} = \begin{pmatrix} 0 & -2 & 0 & 2 \\ -2 & 0 & 0 & -2 \\ 0 & 0 & 0 & 0 \\ 2 & -2 & 0 & 0 \end{pmatrix}$$

Note that all elements w_{3j} and w_{j3} are equal to zero; that is, reactor 3 is uncoupled in this special case. One may write the following coupling scheme.



The electrical currents $G_j(t)$ applied to reactor j via the Pt working electrode are

$$G_1(t) = G_{1in} - w_{21}(\text{Pot}_{2,av} - 1000) + w_{41}(\text{Pot}_{4,av} - 1000)$$

$$G_2(t) = G_{2in} - w_{12}(\text{Pot}_{1,av} - 1000) + w_{42}(\text{Pot}_{4,av} - 1000) \quad (3)$$

$$G_3(t) = G_{3in}$$

$$G_4(t) = G_{4in} - w_{14}(\text{Pot}_{1,av} - 1000) + w_{24}(\text{Pot}_{2,av} - 1000)$$

where G_{jin} (bias) is set equal to 0.45 mA (1.05 mA) for a periodic (nodal) state, $\text{Pot}_{i,av}$ are the averaged redox potentials and w_{ij} are the coupling strengths between reactor i and j . Since the redox potential of the nodal steady state was arbitrarily set equal to 1000 au, the latter must be subtracted from each averaged redox potential in order to establish the nodal steady state as the reference state.

Averaging over a Periodic State. To achieve a transformation from the P to the N state (termed negative coupling), we found it appropriate to use the average of the periodic potential $\text{Pot}_{i,av}$ as input into the $G_j(t)$ equations. To calculate an average value of the periodic potential, the amplitudes of the previous ~ 1.5 oscillations (50 s) were averaged. The averaging process is extended also over the nodal states. It must be sufficiently long to avoid any large periodic fluctuations in $\text{Pot}_{i,av}$.

In the following recognition experiments all experimental w_{ij} values have been empirically set to $-1.25 \mu\text{A}$. This indicates that the contribution of an oscillating reactor i ($\text{Pot}_{i,av} \approx 1400$ arb. units) to the current $G_j(t)$ in reactor j is ca. $-500 \mu\text{A}$ ($(1400 - 1000) \mu\text{A}$) if reactor i and j are positively coupled, while for negative coupling between reactor i and j the term $\sim 500 \mu\text{A}$ is added. There will be no effective contribution of a reactor to the coupling when it is in the nodal steady state ($\text{Pot}_{i,av} = 1000$).

It is well-known that the number of encoded patterns p is limited in a Hopfield net, where $p \approx 0.25x$ (x is the number of neurons).¹¹ Accordingly, only one pattern seems to be formally encoded in the present four-reactor network. However, since reactor 3 is uncoupled, one pattern is encoded in three reactors

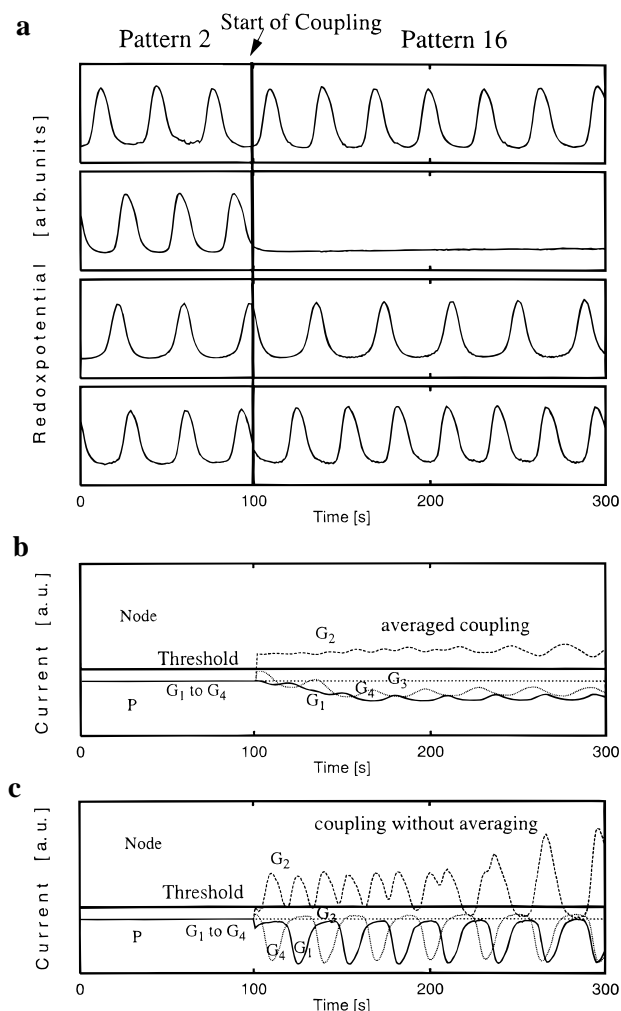


Figure 4. (a) Experimental time series (all four reactors) of the recognition experiment using averaged coupling starting with pattern 2. Pattern 2 is associated with pattern 16 (one error); (b) time course of currents G_1 – G_4 using the averaged redox potentials; (c) the nonaveraged redox potentials in eq 3. The threshold current at the SNIPER bifurcation is indicated as a solid line in b and c.

(and not in four) which is still tolerated by the network. Since reactor 3 will remain either in a P or in a N state as determined by its initial G_{3in} , there are altogether *two* encoded patterns in four reactors.

Results and Discussion

The following experiments briefly discuss the associations of all 14 initial patterns to the encoded patterns 15 and 16 using the coupling equations 3. There are 120 ways to combine 16 patterns in groups of two patterns. We successfully tested a number of these combinations, but they are not reported here owing to space limitations. Phenomenologically, patterns 15 and 16 differ from each other, of course. However, according to the Hopfield matrix, the difference between these two patterns is determined solely by the initial state of reactor 3, which is uncoupled. Since reactor 3 may be either in the N (pattern 15) or P (pattern 16) state, there are 16 different patterns instead of only eight patterns, which might be expected from the entries in the Hopfield matrix.

Recognition of Patterns 1 and 2. As a representative example of this group, pattern 2 shows one error with respect to encoded pattern 16 and two errors with respect to encoded pattern 15 (Figure 3). The main feature in this group is the

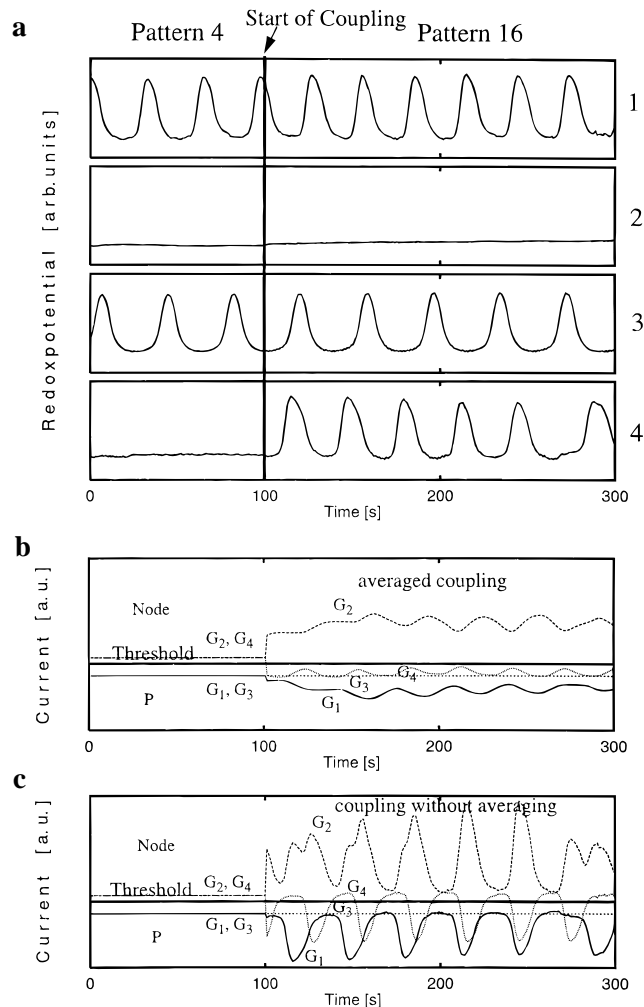


Figure 5. (a) Experimental time series of the recognition experiment using averaged coupling starting with pattern 4. Pattern 4 is associated with pattern 16 (one error); (b) time course of currents $G_1(t)$ – $G_4(t)$ for averaged coupling; (c) for nonaveraged potentials in eq 3. The threshold current at the SNIPER bifurcation is indicated as a solid line in b and c.

transformation of a periodic state into a nodal steady state (reactor 2). In all experiments the coupling interactions are turned on at $t = 100$ s, as shown in the experimental time series (Figure 4a). This transformation can best be visualized from the currents $G_1(t)$ to $G_4(t)$ (Figure 4b). After the start of the coupling interaction, the current $G_2(t)$ crosses the bifurcation point from the P to the N state. Due to the variations of $Pot_{1,av}$ and $Pot_{4,av}$, $G_2(t)$ oscillates while it remains in the nodal steady state. From the bifurcation diagram it is evident (Figure 2) that there is practically no change in the nodal concentration even though $G_2(t)$ oscillates due to its coupling with reactors 1 and 4. It will be observed that reactors 1 and 4 phase-lock as a consequence of the positive coupling $+w_{14}$ ($=w_{41}$) between them. The initial currents $G_1(t)$ and $G_4(t)$ are further lowered due to the negative terms $w_{41}(Pot_{4,av} - 1000)$ and $w_{14}(Pot_{1,av} - 1000)$, respectively. $G_3(t)$ remains constant since reactor 3 is uncoupled. Starting the recognition experiment with pattern 1, the same responses of reactors 1, 2, and 4 are obtained (not shown) if the averaging procedure is employed, and the recognition process results in the encoded pattern 15.

Figure 4c shows the currents when the redox potentials of the periodic state in each reactor are not averaged. It is seen that $G_2(t)$ is shifted to a higher current while it periodically crosses the SNIPER bifurcation after synchronization between

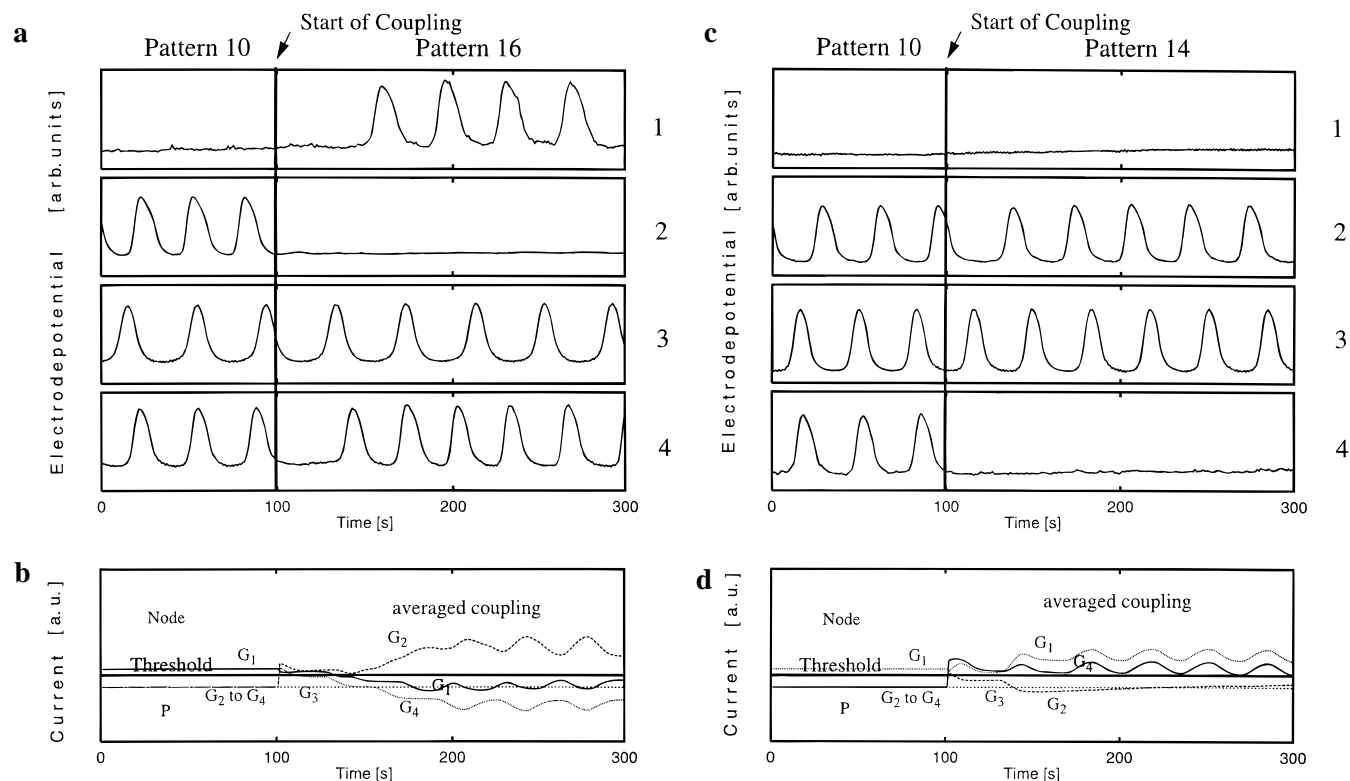


Figure 6. (a and c) Experimental time series; (b and d) time course of electrical currents of recognition experiments with averaged coupling starting with pattern 10. With a 50:50 probability pattern 10 changes either into pattern 16 (two errors) (a) or into pattern 14 (one error) (c); pattern 14 is the mirror image of pattern 15. See Figure 3 and text.

reactors 1 and 4 has taken place. As a consequence, reactor 2 will respond with oscillations instead of the desired nodal steady state. Thus recognition is not possible here without the averaging procedure.

Recognition of Patterns 3, 4, 5, and 6. In this one-error group of patterns a nodal steady state is transferred into a periodic state. For example, pattern 4 shows one error with respect to pattern 16 and two errors with respect to the other encoded pattern 15. The time series of the recognition processes using the averaged redox potentials $Pot_{i,av}$ in eq 3 are shown in Figure 5a for all four reactors using pattern 4 as an initial state. When coupling has been turned on, reactor 4 is transformed from an N into a P state since the current $G_4(t)$ is lowered from the nodal steady state (1.05 mA) to a P state whose current is below 0.85 mA (Figure 5b). $G_2(t)$ is increased while $G_1(t)$ is lowered upon coupling. Coupling *without* averaging also leads to oscillations in reactor 4, since $G_4(t)$ periodically crosses the bifurcation point (threshold) (Figure 5c), which will lead to forced oscillations. In this group of patterns recognition is achieved *with* or *without* averaging. When pattern 3 is used as the initial pattern, a similar behavior of reactors 1, 2, and 4 will be observed, leading to pattern 15 as the recognized pattern.

Patterns 6 and 5 are symmetrical to patterns 4 and 3, respectively, and they display a recognition behavior similar to patterns 4 and 3 (not shown). Patterns 5 and 3 are recognized as pattern 15 (one error), while pattern 6 changes into pattern 16 (one error).

Recognition of Patterns 7, 8, 9, and 10. The behavior of this group of patterns is more complex since they all show two errors with respect to their closest target patterns. For example, pattern 10 has two errors with respect to pattern 16 and three errors with respect to pattern 15. Two different time series for pattern 10 are possible, as shown in Figure 6a,c. After turning on the coupling, pattern 10 changes either into pattern 16 (Figure

6a) or, surprisingly, into pattern 14 (Figure 6c) with a 50:50 probability. In fact, pattern 14 is the mirror image of pattern 15, and the Hopfield matrix represents both the encoded patterns as well as their mirror images. At the start of coupling neither reactor 3 nor reactor 1, which is in a nodal steady state, makes any contribution to the coupling. As a result of the negative coupling between reactors 2 and 4, both reactors transiently approach the nodal state; that is, $Pot_{2,av}$ and $Pot_{4,av}$ decrease, resulting in increased currents $G_2(t)$ and $G_4(t)$ (Figure 6b,d). After a short transience (at ~ 130 s) either reactor 2 (Figure 6c) or reactor 4 (Figure 6a) will change into a periodic state with a 50:50 probability. If, due to fluctuations, reactor 2 accidentally oscillates first, then reactors 1 and 4 remain or end up in the N state, respectively. On the other hand, if reactor 4 oscillates first, then reactor 2 ends up in the N state while reactor 1 shows delayed oscillations due to the positive coupling between reactors 4 and 1. Similar scenarios occur for patterns 3 and 5.

Nonrecognition of Patterns 11 and 12. Patterns 11 and 12 are the only two patterns (two errors) that cannot be recognized since reactors 1, 2, and 4 are all in nodal states; that is, all relevant differences ($Pot_{i,av} - 1000$) are equal to zero (eq 3). This means that there is no interaction between the reactors and local coupling does not come into play. Therefore all reactors in these two patterns will remain in their initial dynamic states; they are dynamically inert.

Pseudorecognition of Patterns 13 and 14. Patterns 14 and 13 are the mirror images of the encoded patterns 15 and 16, respectively. Since mirror images lead to the same Hopfield matrix, patterns 14 and 13 are encoded as well. Thus, if patterns 14 and 13 are offered as initial conditions, there will be no transformation process. This situation may be called pseudorecognition since the mirror images of the encoded patterns are the target patterns in this case. Moreover, a transformation into patterns 16 and 15 is not expected here since three errors

TABLE 1: Seven-Variable Model (Nonstoichiometric Steps)^a

$\text{Br}^- + \text{HBrO}_2 + \text{H}^+$	\rightarrow	2BrMA	(R1)
$\text{Br}^- + \text{BrO}_3^- + 2\text{H}^+$	\rightarrow	$\text{BrMA} + \text{HBrO}_2$	(R2)
2HBrO_2	\rightarrow	$\text{BrO}_3^- + \text{BrMA} + \text{H}^+$	(R3)
$\text{BrO}_3^- + \text{HBrO}_2 + \text{H}^+$	\rightarrow	$2\text{BrO}_2^* + \text{H}_2\text{O}$	(R4)
$2\text{BrO}_2^* + \text{H}_2\text{O}$	\rightarrow	$\text{BrO}_3^- + \text{HBrO}_2 + \text{H}^+$	(R5)
$\text{Ce}^{3+} + \text{BrO}_2^* + \text{H}^+$	\rightarrow	$\text{HBrO}_2 + \text{Ce}^{4+}$	(R6)
$\text{HBrO}_2 + \text{Ce}^{4+}$	\rightarrow	$\text{Ce}^{3+} + \text{BrO}_2^* + \text{H}^+$	(R7)
$\text{MA} + \text{Ce}^{4+}$	\rightarrow	$\text{MA}^* + \text{Ce}^{3+} + \text{H}^+$	(R8)
$\text{BrMA} + \text{Ce}^{4+}$	\rightarrow	$\text{Ce}^{3+} + \text{H}^+$	(R9)
$\text{MA}^* + \text{BrMA}$	\rightarrow	$\text{MA} + \text{Br}^-$	(R10)
2MA^*	\rightarrow	MA	(R11)

^a MA = malonic acid; MA* = malonic acid radical; BrMA = bromomalonic acid.

TABLE 2: Rate Constants and Concentrations of the Seven-Variable Model

k_{R1}	$2.0 \times 10^6 \text{ s}^{-1} \text{ M}^{-2}$	k_{R2}	$2.0 \text{ s}^{-1} \text{ M}^{-3}$
k_{R3}	$3.0 \times 10^3 \text{ s}^{-1} \text{ M}^{-1}$	k_{R4}	$3.3 \times 10^1 \text{ s}^{-1} \text{ M}^{-2}$
k_{R5}	$7.6 \times 10^5 \text{ s}^{-1} \text{ M}^{-2}$	k_{R6}	$6.2 \times 10^4 \text{ s}^{-1} \text{ M}^{-2}$
k_{R7}	$7.0 \times 10^3 \text{ s}^{-1} \text{ M}^{-1}$	k_{R8}	$3.0 \times 10^{-1} \text{ s}^{-1} \text{ M}^{-1}$
k_{R9}	$3.0 \times 10^1 \text{ s}^{-1} \text{ M}^{-1}$	k_{R10}	$2.4 \times 10^4 \text{ s}^{-1} \text{ M}^{-1}$
k_{R11}	$3.0 \times 10^9 \text{ s}^{-1} \text{ M}^{-1}$		
$[\text{BrO}_3^-]$	0.1 M	$[\text{H}^+]$	0.26 M
$[\text{H}_2\text{O}]$	55 M	$[\text{Ce}^{3+}]_0$	$8.33 \times 10^{-4} \text{ M}$
$[\text{MA}]$	0.25 M		

(~75%) would be formally involved in the recognition process that the network cannot overcome.

Recognition of the Encoded Patterns 15 and 16. The presentation of patterns 15 and 16 does not lead to any transformations since patterns 15 and 16 have been encoded and they are immediately recognized (zero error).

Simulations

Model of the Nonlinear Seven-Variable Montanator. To simulate learning and pattern recognition, we use the seven-variable Montanator model,¹⁵ which was developed by Györgyi and Field. The mechanism of the seven-variable model is given in Table 1, and the rate constants and concentrations of the inflow species are given in Table 2. The seven variables of the model are bromous acid, bromide, bromate, bromomalonic acid, bromomalonic acid radical, Ce^{3+} , and Ce^{4+} . The numerical integrations of the differential equations were performed using the Gear method.^{16,17} We simulate the effect of the electric current by adding the term $+C[\text{Ce}^{4+}]$ to the rate equation for $[\text{Ce}^{3+}]$ and by adding the negative term $-C[\text{Ce}^{4+}]$ to the rate equation of $[\text{Ce}^{4+}]$:

$$\frac{d[\text{Ce}^{3+}]}{dt} = f([\text{Ce}^{3+}]) - k_t([\text{Ce}^{3+}] - [\text{Ce}^{3+}]_0) + C[\text{Ce}^{4+}]$$

$$\frac{d[\text{Ce}^{4+}]}{dt} = f([\text{Ce}^{4+}]) - k_f[\text{Ce}^{4+}] - C[\text{Ce}^{4+}]$$

where C is a parameter that is proportional to the amount of charge delivered at the Pt working electrode. The inflow concentration of Ce^{3+} is given by $[\text{Ce}^{3+}]_0$ and $f([\text{Ce}^{3+}])$ contains the rate equation of the model (Table 1). The bifurcation diagram with the electric current C as the bifurcation parameter is shown in Figure 7. P1 oscillations occur from $C = 0$ to $C = 0.11$. A SNIPER bifurcation is observed at $C = 0.11$, beyond which a nodal steady state exists.⁴ To obtain P1 oscillations in the free running mode without electric current, a flow rate of $k_t = 3.5 \times 10^{-4} \text{ s}^{-1}$ was chosen. The semiquantitative agreement with the experimental bifurcation diagram (Figure 2) is sufficient

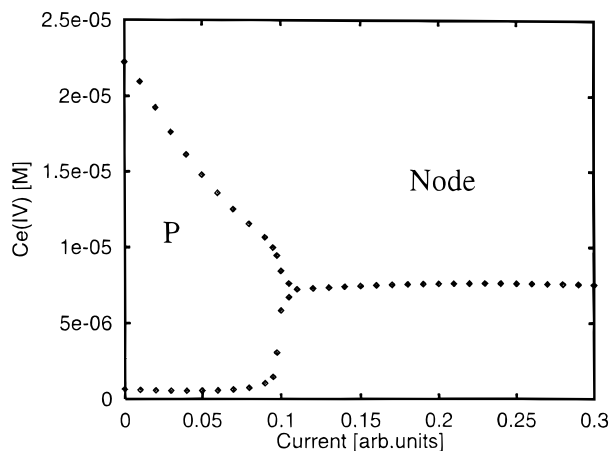


Figure 7. Calculated bifurcation diagram for Ce(IV) of the seven-variable Montanator model. The electrical current C is the bifurcation parameter. The oscillations P change into a node N at the SNIPER bifurcation at $C = 0.11$.

to realistically model the effect of the electric current in the learning and recognition phases.

Recognition of Pattern 5. All recognition calculations for the encoded patterns 15 and 16 and other pattern combinations were carried out successfully, but they are not shown here. However, as a representative example, we offer pattern 5 as the initial pattern to demonstrate recognition in the simulations of the four coupled reactors (eq 3). Pattern 5 shows one error with respect to pattern 15 and two errors with respect to pattern 16. Recognition involves the conversion of an N state in reactor 1 to a P state. When coupling was turned on at 5000 s (Figure 8) in the simulations, it was immediately obvious that coupling *without averaging* the Ce^{4+} concentrations does not lead to recognition of pattern 15 since reactor 2 is in the P and not in the N state. Furthermore, reactors 1 and 2 show oscillations with small amplitudes due to the oscillations of the current after coupling has been started. Recognition can be easily achieved, however, by averaging over the Ce^{4+} concentrations in the P states (Figure 9). It is important to note that this average value lies somewhat below the nodal steady state in the model, whereas in the experiments the average is *above* the experimental nodal steady state. The reference state in the simulations is also the nodal steady state whose value is $7.79 \times 10^{-6} \text{ M}$ (e.g., Figure 8) as compared with 1000 arbitrary units assigned to the nodal steady state in the experiments. Thus the w_{ij} values carry opposite signs in the simulations as compared with the experiments. It is noted that coupling equations in the simulations are identical with the coupling equations in the experiments (eqs 3). Thus, when coupling is started (Figure 9), the current in reactor 1 declines from $C = 0.12$ (steady state) to $C = 0.091$ (P1 oscillations, $T = 480 \text{ s}$) (Figure 9b). These oscillations are stabilized after a transient time of ~1500 s. Reactors 2 and 3 remain in the nodal state; reactor 4 remains in the P state ($t = 180 \text{ s}$). It is seen that the frequency in reactor 1 is lower than that in reactor 4. The reason is the difference in the currents C_1 and C_4 , where $C_4 < C_1$. In the SNIPER scenario higher currents always lead to lower frequencies. The average of $[\text{Ce}^{4+}]$ has been calculated using all oscillations in the time series. Pattern recognition is not successful in the simulations if the average is calculated only from a small number of oscillations.

Interactive Gaussian Noise. To realistically simulate an experiment, we added Gaussian distributed noise to the model in the recognition process. This was done by adding interactive noise to all seven variables. As a result, Gaussian distributed

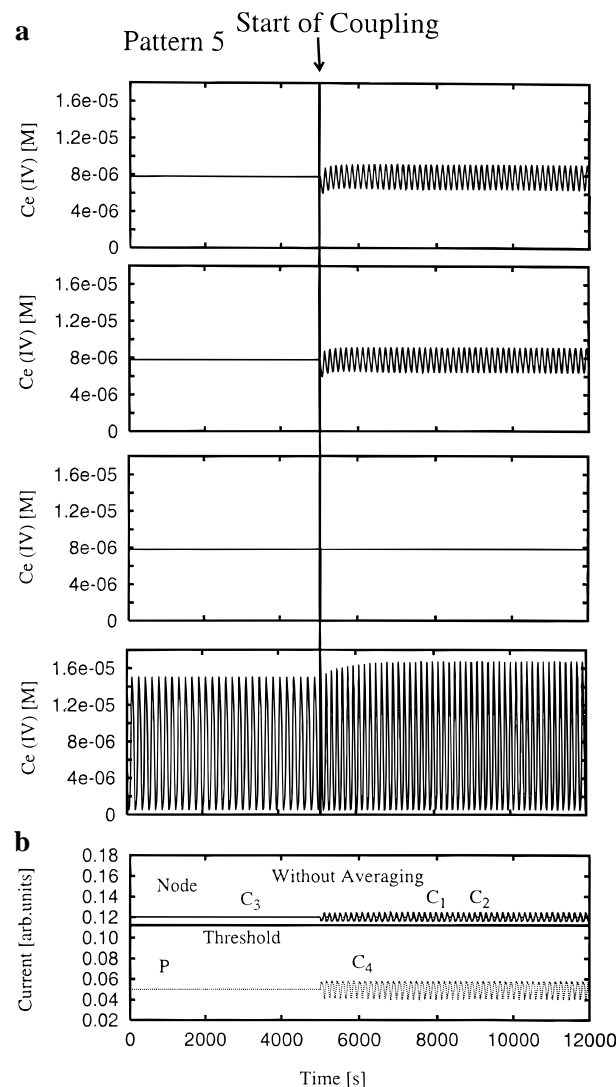


Figure 8. (a) Simulated time series and (b) currents C_1 – C_4 describing the recognition process starting with pattern 5. The nonaveraged Ce(IV) concentrations lead to nonrecognition.

noise leads to recognition of patterns 15 and 16 only if the standard deviation (D) is less than 1×10^{-4} (Figure 10). Gaussian noise of $D \geq 10^{-4}$ leads to nonrecognition.

Learning Process. *Learning Iteratively without Noise.* In a traditional Hopfield network, learning is carried out in a single step by constructing the Hopfield matrix according to the rules of eqs 1 and 2 without any later changes in the matrix elements. In contrast, here we simulate the learning process by iterative presentations of patterns to be encoded. With each iteration step a small increment Δw_{ij} is added to the relevant elements of the Hopfield matrix starting from zero. For patterns 15 and 16 to be encoded we chose $\Delta w_{ij} = 200$ arb. units to iteratively build up their Hopfield matrix. In the computer experiment we use pattern 5 as a test pattern for recognition, which involves the transformation of reactor 1 from an N to a P state. We found that recognition was achieved at the 110th iteration. At iteration 109 and below recognition was completely absent. Recognition occurred at all steps above 109 iterations. Thus the elements in the Hopfield matrix reached their critical values for recognition at iteration 110. The critical value of w_{ij} for recognition is therefore 22 000 arb. units ($=200 \times 110$) in the simulations. The choice of lower values of Δw_{ij} was also tested; as a result, more iterations were required for recognition. Therefore, in the absence of any noise, recognition occurs

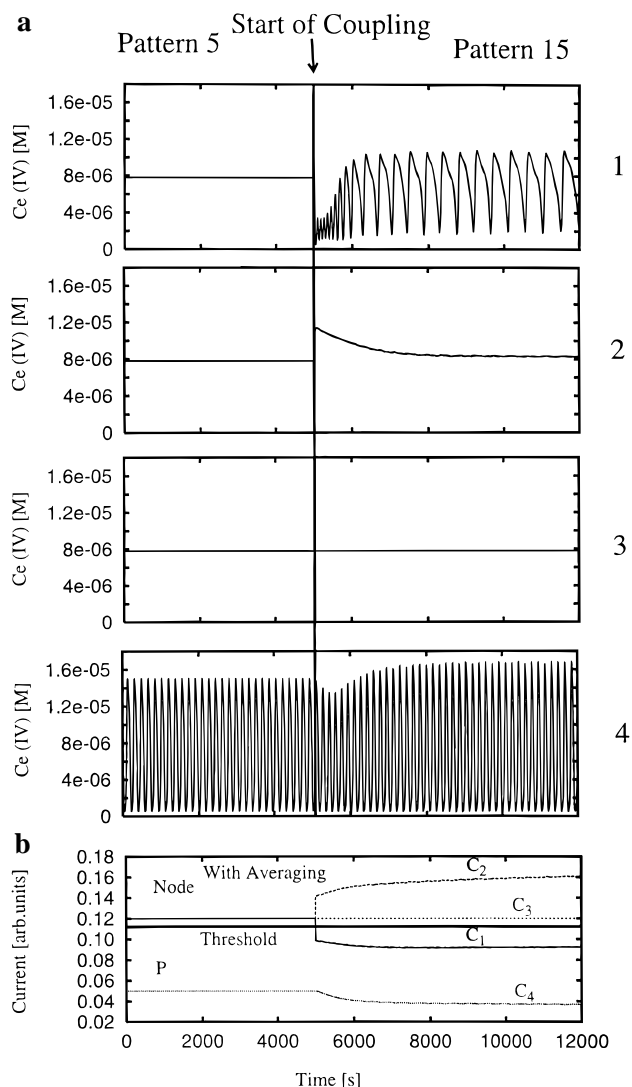


Figure 9. (a) Simulated time series using averaged coupling for pattern 5, leading to recognition of pattern 15; (b) currents C_1 – C_4 for the recognition process in a starting with pattern 5.

abruptly in a stepwise fashion at a certain threshold in this small model network. This situation is analogous to a first-order phase transition. However, when parameter noise is added to the coupling strengths, the recognition curve broadens.

Learning Iteratively with Parameter Noise. To study the effect of noise, we added parameter noise of a normal distribution to all elements of the Hopfield matrix. Starting from randomized elements (synapses) the increments Δw_{ij} and $R\xi$ were added to the elements of the matrix for patterns 15 and 16 at each learning iteration. ξ is equally distributed between +1 and -1. The noise varied in each of the ranges (R) 1000, 1500, 3000, and 5000 arb. units (Figure 11). For every learning iteration the average recognition probability is plotted versus the number of iterations, where each point represents an average of 200 numerical calculations.

For noise levels of 1000 arb. units the recognition curve is broadened and 100% recognition is no longer achieved (Figure 11). In fact, for large numbers of iterations (~ 350) the recognition curve declines due to the accumulation of noise in the Hopfield matrix. For noise of R 1500 and 2000 arb. units the recognition curve shows a similar but more pronounced behavior: a steeper increase and a lower maximum is observed at a lower number of iterations. Finally, very large noise (3000 and 5000 arb. units) dramatically affects learning and recogni-

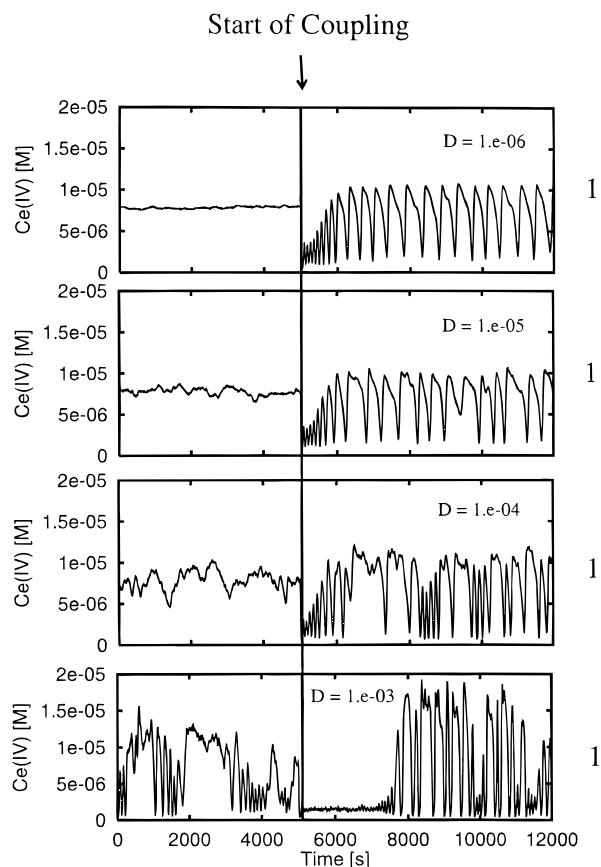


Figure 10. Time series of reactor 1 with Gaussian-distributed interactive noise imposed on all seven variables, where pattern 5 is offered as initial pattern. Gaussian-distributed noise is added to all seven variables of the Montanator model. Nonrecognition is observed for $D \geq 1 \times 10^{-4}$.

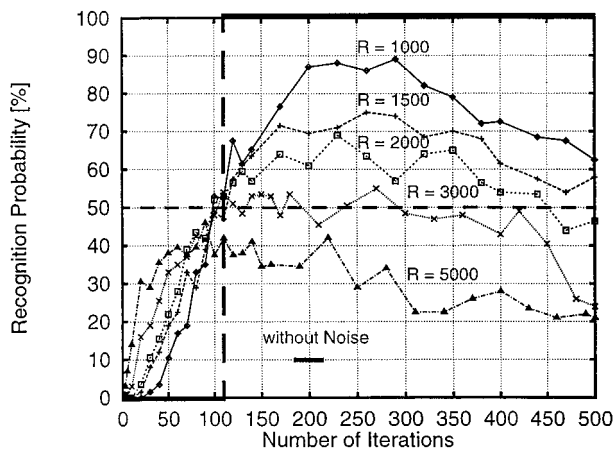


Figure 11. Recognition curve for iterative learning with $\Delta w_{ij} = 200$ arb. units with parameter noise of $R = 0, 1000, 1500, 2000, 3000,$ and 5000 arb. units without interactive noise. Learning without or with very small parameter noise (solid line) leads to a sharp “phase transition” at the 110th iteration. The recognition curve for very small parameter noise ($R = 10$ arb. units, not shown) is indistinguishable from $R = 0$. For increasing noise ranges the recognition curves become broader and their maxima are lower. Time required to simulate one point: 2–3 days.

tion. Although the first iteration already produces recognition in a few percent of the 200 recognition simulations, the recognition curve does not even reach the 50% mark ($\sim 40\%$ recognition at ~ 70 iterations for 5000 arb. units), and it declines rapidly to zero due to the effective randomization of all elements in the Hopfield matrix. The latter decline may be called

“forgetting”. In the latter case a large number of iterations is detrimental to the learning process. Thus noise seems to be advantageous in the early stages of learning but disadvantageous in the later stages. In all cases noise reduces the maximum attainable recognition probability from unity, which is reached in a noise-free system.

Conclusions

Two patterns were encoded in a small chemical reactor network consisting of four reactors that were coupled according to a Hopfield net. A single reactor can assume either a periodic (P) state or a nodal (N) state in the BZ reaction where the bifurcation between the two states is relatively sharp (SNIPER bifurcation). Other “sharp” bifurcations (e.g., subcritical Hopf bifurcation) would also be suitable to carry out recognition processes. The bifurcation parameter is the electrical current that leads to redox processes on the Pt working electrodes. Local coupling between the reactors also occurs by the electrical current. The present recognition experiments are carried out without global coupling. Problems arise in general if negative and positive couplings occur simultaneously in a small network. The use of an averaged oscillatory signal makes it possible to circumvent this problem at the expense of any phase information. There are 16 ($=2^4$) different reactor states with 120 possible combinations, of which two are selected (patterns 15 and 16) as the patterns to be encoded in the experiments described here. The experimental network is capable of associating all remaining (14) patterns with the two encoded patterns except for patterns 11 and 12, which are nonrecognizable, since they are dynamically inert. Patterns 13 and 14 are also encoded since they are mirror images of the two encoded patterns 15 and 16. In computer simulations we are able to reproduce all experiments by the use of the Györgyi–Field model for the BZ reaction. Interactive noise reduces the recognition capability of the network. To our knowledge we present a novel iterative learning procedure in building up the elements in the Hopfield matrix without any back-propagation of errors. The iterative learning method is tested by the calculation of a recognition curve which resembles a sharp first-order phase transition in this small network in the absence of parameter noise or interactive noise. When parameter noise (without interactive noise) is included in the iterative learning process, the recognition curve is broadened and the maximum recognition probability declines dramatically. It is observed that a large amount of parameter noise leads to an early rise in the recognition probability at the cost of a substantially reduced maximum in the recognition curve. Thus parameter noise augments the recognition process in the early stages of learning, whereas it reduces recognition in its later stages.

It is noted that mass coupling is restricted to positive coupling, and only those few patterns that are characterized by positive coupling may be recognized.⁸ On the other hand, the present electrical coupling method together with the averaging procedure is capable of performing positive as well as negative coupling, since electrical currents can be added or subtracted. The averaging procedure removes any phase information which, however, is not critical for the present recognition experiments. Reactor networks consisting of eight electrically coupled reactors are under investigation.

Acknowledgment. We thank the Deutsche Forschungsgemeinschaft and the Fonds der Chemischen Industrie for financial support of this work.

References and Notes

- (1) Zeyer, K.-P.; Dechert, G.; Hohmann, W.; Blittersdorf, R.; Schneider, F. W. *Z. Naturforsch.* **1994**, 49A, 383.
- (2) Steinbock, O.; Kettunen, P.; Showalter, K. *J. Phys. Chem.* **1996**, 100, 18970.
- (3) Dechert, G.; Zeyer, K.-P.; Lebender, D.; Schneider, F. W. *J. Phys. Chem.* **1996**, 100, 19043.
- (4) Hohmann, W.; Kraus, M.; Schneider, F. W. *J. Phys. Chem.* **1997**, 101, 7364.
- (5) Hjelmfelt, A.; Weinberger, E. D.; Ross, J. *Proc. Natl. Acad. Sci. U.S.A.* **1991**, 88, 10983; **1992**, 89, 383.
- (6) Hjelmfelt, A.; Schneider, F. W.; Ross, J. *Science* **1993**, 260, 335.
- (7) Hjelmfelt, A.; Ross, J. *J. Phys. Chem.* **1993**, 97, 7988.
- (8) Laplante, J.-P.; Pemberton, M.; Hjelmfelt, A.; Ross, J. *J. Phys. Chem.* **1995**, 99, 10063.
- (9) Hanyu, Y.; Matsumoto, G. *Physica* **1991**, D49, 198.
- (10) Hopfield, J. J. *Proc. Natl. Acad. Sci. U.S.A.* **1982**, 79, 2554; **1984**, 81, 3088.
- (11) Zupan, J.; Gasteiger, J. *Neural Networks for Chemists*; VCH Verlag: Weinheim, 1993.
- (12) Hebb, D. O. In *Neurocomputing: Foundations of Research*; Anderson, J. A., Rosenfeld, E., Eds.; MIT Press: Cambridge, 1988.
- (13) Rumelhart, D. E.; Hinton, G. E.; Williams, R. J. *Nature* **1986**, 323, 533.
- (14) Lebender, D.; Müller, J.; Schneider, F. W. *J. Phys. Chem.* **1995**, 99, 4992.
- (15) Györgyi, L.; Field, R. J. *J. Phys. Chem.* **1991**, 95, 6594; *Nature* **1992**, 355, 808.
- (16) Gear, C. W. *Numerical Initial Value Problems in Ordinary Differential Equations*; Prentice Hall: Englewood Cliffs, NJ, 1971.
- (17) Shampine, L. F.; Gear, C. W. *SIAM Rev.* **1979**, 21, 1.